ISSN 1068-1620, Russian Journal of Bioorganic Chemistry, 2015, Vol. 41, No. 2, pp. 161–169. © Pleiades Publishing, Ltd., 2015.
Original Russian Text © H.Q. Nguen, K.A. Zhdanova, V.S. Uvarova, N.A. Bragina, A.F. Mironov, V.V. Chupin, V.I. Shvets, 2015, published in Bioorganicheskaya Khimiya, 2015, Vol. 41, No. 2, pp. 185–194.

Development and Characterization of Nanoparticles Prepared from the Mixture of Triterpenoids and Amphiphilic *meso*-Arylporphirins

H. Q. Nguen[a], K. A. Zhdanova[a, b], V. S. Uvarova[a], N. A. Bragina[a], A. F. Mironov[a], V. V. Chupin[b, 1], and V. I. Shvets[a]

[a] *Moscow State University of Fine Chemical Technologies, pr. Vernadskogo 86, Moscow, 119571 Russia*
[b] *Moscow Institute of Physics and Technology, Institutskii per. 9, Dolgoprudnyi, 141700 Russia*

Received February 17, 2014; in final form, October 16, 2014

Abstract—The mixture of triterpenoids from birch bark and amphiphilic *meso*-arylprophyrins was used to develop spherical amorphous nanoparticles. The nanoparticles were studied with the methods of electron microscopy, dynamic light scattering, UV spectroscopy, and fluorimetry. The efficiency of incorporation of a porphyrin sensitizer into the nanoparticles and the possibility to use them as a drug delivery vehicle were demonstrated.

Keywords: amphiphilic meso-arylporphyrins, spherical amorphous nanoparticles, birch bark triterpenoids, photosensitizers, photodynamic therapy

DOI: 10.1134/S1068162015020107

Development of new systems for targeted delivery of therapeutic and diagnostic agents is one of the fields of modern studies. Today, the following systems for delivery of hydrophobic agents have been elaborated: liposomes [1], microcapsules [2], lipoproteins [3], micelles [4, 5], nanoparticles [6], etc. Their utilization is aimed at increased bioavailability and efficiency through targeted effects in pathological zones, prevention of negative side effects, and decreased cytotoxicity for normal cells.

The approach is of interest for photodynamic therapy (PDT) as well, since most of photosensitizers (PSs) are derivatives of hydrophobic tetrapyrrole compounds [7]. Incorporation of such PSs into nanostructures allows for decreasing their side effects upon utilization as therapeutic agents, increasing solubility and dispersion. The relative efficiency and intercellular localization of tetrapyrrole PSs are predetermined by the structure and, particularly, amphiphilic properties of the molecule and the type and arrangement of hydrophilic and hydrophobic substituents around the tetrapyrrole macrocycle [8–10]. The easily available synthetic porphyrins actively explored today are analogues of natural PSs [11–14].

The actively studied hydroxysubstituted porphyrins are structural analogues of a second generation PS, *meso*-tetrahydroxyphenylchlorine (*m*-THPC) used in clinics under trade name Foscan®. The problems of low solubility of PSs and inefficient internalization by cells can be solved by introduction of hydrophilic substituents (hydroxy, sulfate, and phosphate groups, PEG) into the macrocycle or binding of peptides, sugars, cyclodextrins, etc. [15–18]. There are reports on the possibility to use PEG conjugates of porphyrins for treatment of various diseases, including PTD of cancer. Hydrophilic PEG-based polymers make therapeutic agents more stable spatially, invisible to mononuclear phagocytes and opsonizing proteins (immunoglobulins and complement factors), decrease toxicity, immunogenicity, and allergenic potency of drugs, and increase their lifetime in blood serum [20, 21].

RESULTS AND DISCUSSION

Earlier, the efficiency of spherical amorphous nanoparticles (SANPs) prepared from the major components of birch bark triterpenoid mixture (BTM) as immunological adjuvants, as well as drug delivery systems for hydrophobic compounds (doxorubicin, rifampicin, rifabutin, diclofenac, etc.) has been demonstrated [22, 23]. SANPs (average size of 100–200 nm) are not toxic and, owing to their structural features,

Abbreviations: CHS, cholesteryl hemisuccinate; DDQ, 2,3-dichloro-5,6-dicyano-1,4-benzoquinone; DMF, dimethylformamide; SDS, sodium dodecyl sulfate; TEG, triethylene glycol; THF, tetrahydrofuran; PEG, polyethylene glycol; SANP, spherical amorphous nanoparticles; BTM, birch bark triterpenoid mixture; PDT, photodynamic therapy; PS, photosensitizer.

[1] Corresponding author: phone: +7 (962)-224-40-20; e-mail: vvchupin@gmail.com.

can be used as drug delivery vehicles for hydrophobic compounds. The major components of BTM are triterpenoids of the lupan series: betulin, lupeol, and betulinic coffeate (Formulas 1).

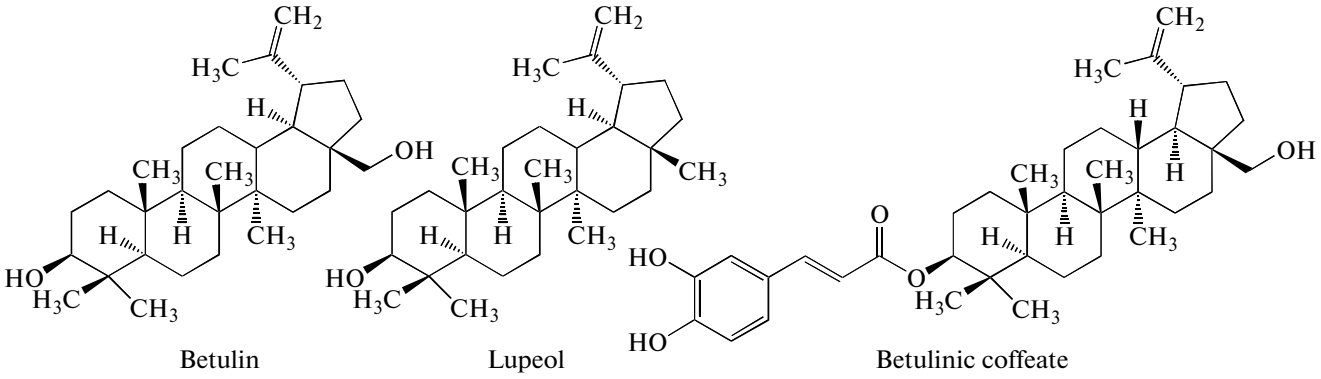

Formulas 1. The major components of treiterpenoids of birch bark.

The aim of the study was to improve water solubility of model amphiphilic drugs (synthetic *meso*-arylporpyrins) through incorporation into SANPs of BTM and investigate the behavior of such nanoparticles as potential agents for PTD. A series of porphyrins (**I**)–(**V**) (Formulas 2) with varying degree of hydrophobicity of substituents and their position in the tetrapyrrole cycle has been synthesized and the methods of incorporation of the synthesized *meso*-arylporphyrins in SANPs have been elaborated. It should be noted that compounds (**I**)–(**V**) are not soluble in water, while nanoparticles with incorporated porphyrins are water-soluble.

Synthesis of Porphyrins (I)–(V)

Tetraphenylporphyrin (**I**) and porphyrins (**II**)–(**IV**) were synthesized according to previously published techniques ([24] and [25], respectively). Earlier, PEG-conjugated porphyrins were prepared according to [26] through alkylation of 5,10,15,20-(4-hydroxyphenyl)porphyrin with methoxypolyethylene glycol mesylate. In the current work, we propose an alternative approach to synthesis of porphyrin (**V**), that is, the monopyrrole condensation in an aqueous micellar system, which allows for high yields of porphyrins with labile functional groups [25, 27]. For synthesis of porphyrin (**V**) (scheme), the initial 4-{2-[2-(2-methoxyethoxy)ethoxy]ethoxy}benzaldehyde (**VI**) was prepared

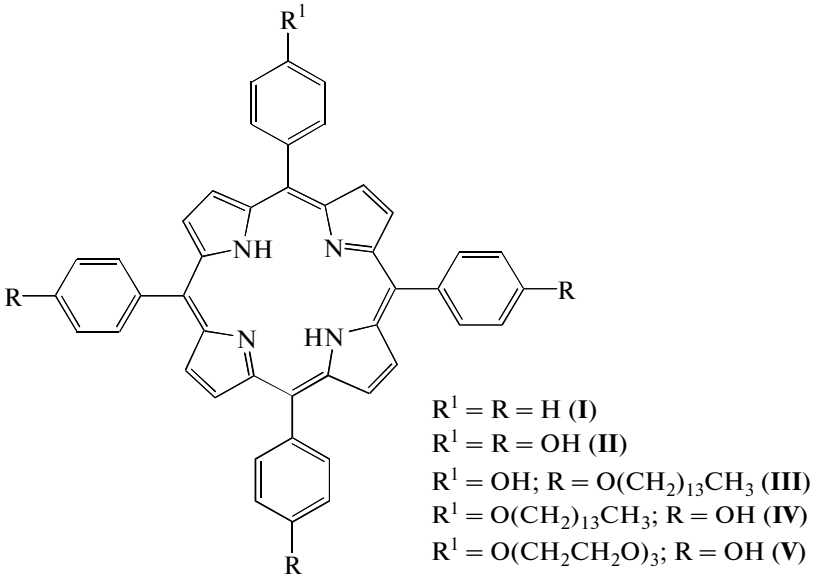

Formulas 2. Structures of porphyrins under study.

according to a published technique [26] by synthesis of 1-(4-methylsulfonyl)-3,6,9-trioxodecane and introducing the product into reaction of *p*-hydroxybenzaldehyde *O*-alkylation in boiling DMF in the presence of Cs_2CO_3. The benzaldehyde derivative (**VI**) yield was 80–85%. Purity and structure of the aldehyde was confirmed by TLC, IR, ^1H, ^{13}C NMR spectra, and LC-MS. A characteristic band of aldehyde group C=O bond valence vibrations (1693 cm^{-1}) was present in the IR spectrum.

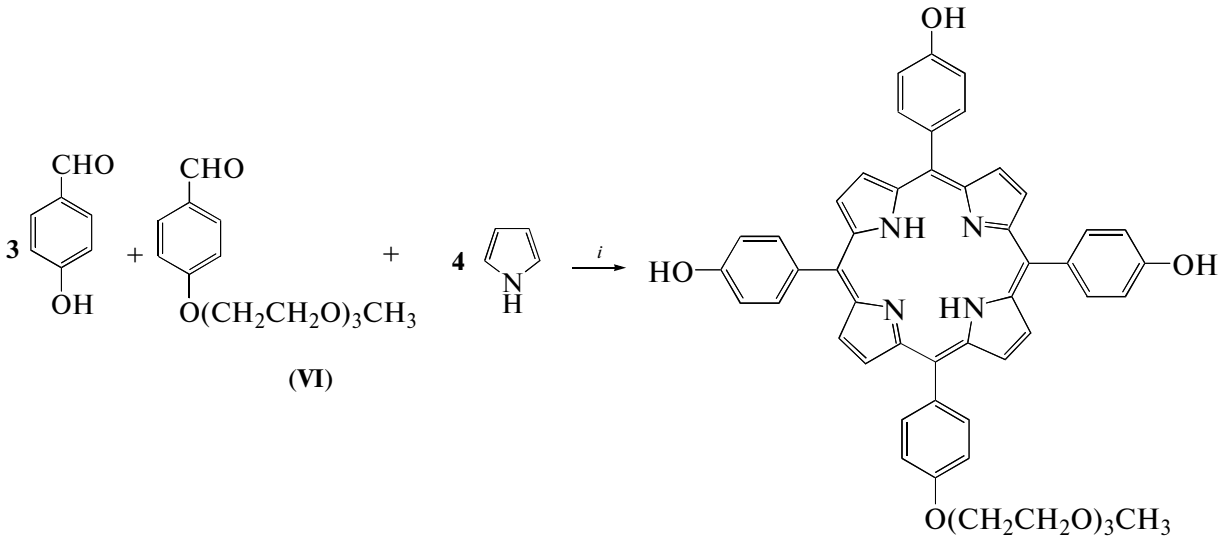

(**VI**)

(**V**)

Reagents and conditions: *i* – C_2H_5COOH, CH_3COOH, $C_6H_5NO_2$, *t*°C

Scheme 1. Synthesis of porphyrin (**V**).

The reaction of mixed aldehyde condensation (molar ratio between *p*-hydroxybenzaldehyde, benzaldehyde (**VI**), and pyrrole of 3 : 1 : 4) was performed in 0.5 M SDS solution (Scheme 1). Hydrochloric acid (2%) was used as catalyst and DDQ, as oxidizing agent. Reaction time was 1 h. To isolate the target product (**VI**), SDS was transformed into a potassium salt insoluble in organic solvents, and the porphyrin was extracted with ethyl acetate and purified by silica gel chromatography using the mixture of methylene chloride–ethyl acetate, 2 : 1. The first fraction was a symmetric porphyrin (**I**) with the yield of 10% and the second one was 5-{4-2-[2-(2-methoxyethoxy)ethoxy]oxyphenyl}-10,15,20-tris(4-hydroxyphenyl)porphyrin (**V**) with the yield of 8%.

Thus, monopyrrole condensation in aqueous micellar system allowed successful synthesis of a new porphyrin (**V**); the technique of preparation and isolation of the porphyrin was optimized.

The formation of the porphyrin system in compounds (**I**)–(**V**) was confirmed by the data of electronic absorption spectroscopy. There is a Cope band at 420 nm and four absorption bands in the absorption spectrum at the border between the UV and visible region (the *ethio* type of spectrum). Purity and structure of the obtained compounds (**I**)–(**V**) were confirmed by the data of TLC, IR, ^1H, and ^{13}C NMR spectra, and mass spectrometry.

Nanoparticle Size Determination

The size of SANPs modified with porphyrins (**I**)–(**V**) was determined by the method of laser light scattering. To modify SANPs with porphyrins, the optimal ratio between the mixture of birch bark triterpenoids (BTM) and the modifying agent (porphyrin) was to be found. Series of nanodispersions of BTM modified under the following conditions: (1) under fixed concentration of porphyrins (2%) with varying cholesterol hemisuccinate (CHS) content (0, 1, and 5% to the BTM mass) and (2) under fixed concentration of CHS (2%) and varying concentration of porphyrins (0, 5, and 10% to the BTM mass) (Table 1). Particle size for most of the compounds was in the range of 100–200 nm, which is acceptable for nanopreparations. Under fixed concentration of porphyrins (series 1), particle size gradually decreases with increasing concentration of CHS. At the highest CHS concentration (5%) and porphyrin (**II**)–(**V**) concentration of 2% (except for tetraphenylporphyrin), nanoparticles were the smallest. In the second series of experiments, at fixed CHS concentration (2%), particle size gradually increased

Table 1. Size of SANPs with incorporated porphyrins obtained at constant percent of porphyrins and varying percent of CHS (experimental series 1) and at constant percent of CHS and varying percent of porphyrins (series 2)

Compound	Series 1			Series 2		
	porphyrin, %	CHS, %	particle size, nm	porphyrin, %	CHS, %	particle size, nm
(I)	0	0	176	–	–	–
	2	0	216	–	–	–
	2	1	407	–	–	–
	2	5	408	–	–	–
(II)	0	0	176	–	–	–
	2	0	238	0	2	193
	2	1	213	5	2	246
	2	5	166	10	2	305
(III)	0	0	176			
	2	0	327	0	2	193
	2	1	286	5	2	277
	2	5	217	10	2	280
(IV)	0	0	114			
	2	0	143	0	2	193
	2	1	151	5	2	176
	2	5	158	10	2	160
(V)	0	0	176			
	2	0	185	0	2	193
	2	1	260	5	2	152
	2	5	175	10	2	202

upon increase in the concentration of loaded compounds and reached the largest sizes at porphyrin concentration of 10% (Table 1). Figure 1b presents the data on particle size for compound **(V)** at the porphyrin concentration of 10%.

Zeta Potential (ζ) Determination

The next stage was to determine the ζ-potential of the prepared dispersions. The results are presented in Table 2. Values of ζ-potential of the dispersions are in the range from −33 to −37 mV. For example, Fig. 1a demonstrates ζ-potential values for compound **(V)**. ζ-Potential values of nanodispersions increased with increasing hydrophobicity of porphyrins loaded in SANPs in the following order: **(V)** < control (SANPs without porphyrins) < **(II)** < **(IV)**. Supposedly, the major role in stabilization of SANP dispersions is played by betulinic coffeate, pyrocatequine groups of which create a negative charge preventing aggregation of the nanoparticles. At relevant pH values, negatively charged ions of betulinic coffeate (mainly, OH^-), as a rule, dissociate and migrate to the nanoparticle surface creating a negative potential layer around the particles. In the course of SANP formation, charged molecules are to be pushed out to the surface of the particles, imparting them with a negative charge. This surface charge, in turn, prevents aggregation of SANPs.

Nanoparticle Morphology

Nanoparticle morphology was studied with the electron microscopy. Figure 2 presents the microphotographs of SANPs modified with porphyrins **(IV)** and **(V)**, as well as the control dispersion containing no porphyrins. There are three types of components in all microphotographs: spherical nanoparticles, small dispersed rod-like crystals, and gray suspended regions.

Nanoparticles have equal size, are isolated and do not aggregate. Comparison of the control nanodispersion and the obtained dispersions (with porphyrin **(IV)** and **(V)** concentration of 10%) allows us to conclude that gray suspended regions are produced by choles-

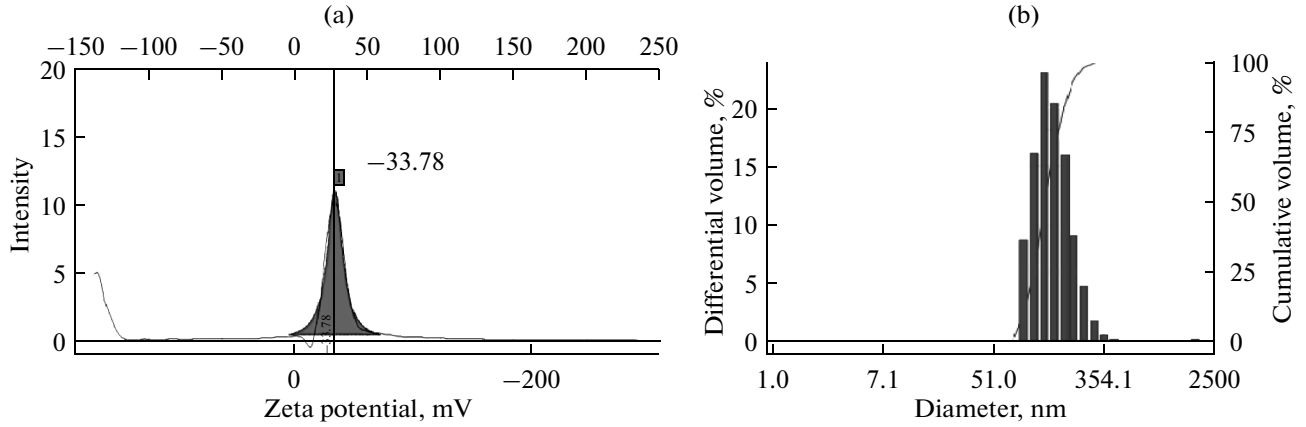

Fig. 1. Characteristics of SANPs loaded with 10% of porphyrin (**V**) and 2% CHS: (a) zeta-potential and (b) size of the particles according to the data of dynamic light scattering.

teryl hemisuccinate and the rod-like crystals of smaller size are the remnants of birch bark triterpenoids not forming the nanostructures (betulin and lupeol). The observed spherical vesicles are nanoparticles formed by betulinic coffeate. Therefore, porphyrin molecules and SANPs form stable spherical agglomerates; however, the question of precise localization of porphyrin molecules in SANPs (encapsulation inside the particles or adsorption on their surface) remains open.

Based on the data on the nanoparticle size and morphology, we studied the amount of porphyrins incorporated in the nanoparticles using UV spectroscopy and fluorimetry. According to our experimental data, amphiphilic *meso*-arylporphyrins efficiently bind the birch bark triterpenoid nanoparticles. The particles are of spherical shape and small size, rather evenly spread in the nanodispersion. The addition of cholesteryl hemisuccinate increases the dispersion stability and the amount of porphyrins loaded in the nanoparticles.

Nanoparticles with porphyrins with the highest concentration of CHS (5%) are the smallest. Study of electron absorption spectra (EAS) demonstrated that at fixed concentration of loaded compounds (**I**)–(**V**) (2%), increase in CHS concentration to 5% promotes the porphyrin loading in the nanoparticles. The results of fluorimetry of porphyrins (**IV**) and (**V**) demonstrate that the addition of CHS resulted in increased intensity of fluorescence, reaching the peak at 5% CHS (Figs. 3b, 4b). On the contrary, at fixed concentration of CHS (2%) (Figs. 3a, 4a), an increase in the concentration of porphyrins to 10% led to a decrease in the intensity of fluorescence if compared to a lower concentration (5%). Such a decrease in the fluorescence intensity is a result of porphyrin aggregate formation.

To prove the formation of porphyrin–SANP nanoparticles, we conducted an experiment on the measurement of fluorescence of the initial porphyrin in an organic solvent and compared the result with the spectra of the nanoparticles. When porphyrin–SANP nanoparticles were formed, fluorescence was quenched if compared with free porphyrin in THF. Upon nanoparticle disruption with sodium dodecyl sulfate (SDS), fluorescence of porphyrin was restored, which proved its release from the porphyrin–SANP particles. The experiment was performed at two concentrations of porphyrin (**V**): 0.005 mg/mL (1%) and 0.01 mg/mL (2%). At porphyrin (**V**) concentration of 1% only approximately 50% of the porphyrin was released into the dispersing medium upon particle disruption, and at a concentration of 2%, almost 100% (Fig. 5).

Therefore, new nanoparticles were produced based on a series of synthesized amphiphilic *meso*-arylporphyrins (**I**)–(**V**) and birch bark triterpenoids; their characteristics were investigated. The nanoparticles are stable, water-soluble, and are 100–200 nm in diameter. Cholesteryl hemisuccinate (CHS) increases the dispersion stability and the loading of the nanoparticles with the porphyrins. The efficiency of porphyrin sensitizer incorporation into the nanoparticles and the possibility of use of the nanoparticles as a delivery vehicle for hydrophobic drugs was demonstrated. The nanoparticles are potential agents for photodynamic therapy. We plan to continue biological studies of the nanoparticles.

Table 2. Zeta potential of SANP dispersions under study

Zeta potential of SANP dispersions under study, mV	
Control (SANP without CHS and porphyrins)	−34.58
CHS + 2% CHS + 10% porphyrin (**II**)	−35.09
CHS + 2% CHS + 10% porphyrin (**IV**)	−36.29
CHS + 2% CHS + 10% porphyrin (**V**)	−33.78

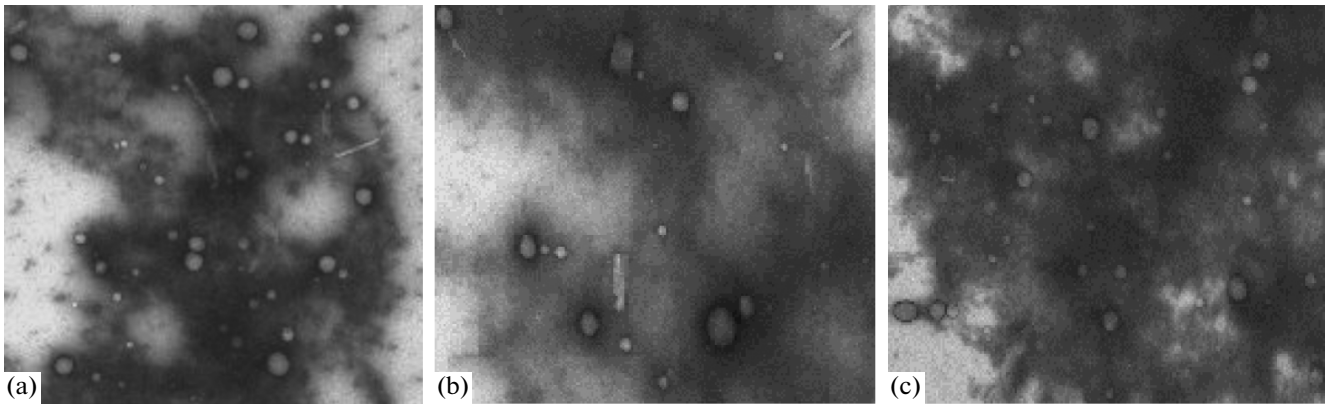

Fig. 2. Electron microscopy images of dispersions of SANPs loaded with (a) 2% CHS and 10% porphyrin (**V**), (b) 10% porphyrin (**IV**), and (c) 2% CHS without porphyrins (control). Scale bar is 140 nm.

EXPERIMENTAL

In the work we used the following commercial reagents and solvents: BTM (OOO Beryozovyi mir, Russia) (60 ± 5% betulin, 30 ± 4% lupeol, and 9 ± 3% betulinic coffeate), cholesteryl hemisuccinate (≥99%) (Sigma-Aldrich), cesium carbonate (Sigma), sodium dihydrophosphate, sodium hydrophosphate, tetrahydrofuran (Khimmed), calcium hydride, phosphorus pentoxide, *p*-hydroxybenzaldehyde, pyrrole, benzaldehyde, mesyl chloride, silica gel G60 (Merck). Distilled water used to prepare the buffer for nanodispersions was filtered through 220-nm filters (MPN pore, United States). Methylene chloride was distilled over calcium chloride and pyrrole, over calcium hydride.

IR spectra of the compounds were recorded on an Infralum FT-02 (NPF AP Lumex, Russia) FT IR spectrophotometer in the range of 4000–600 cm^{-1} with the resolution of 1 cm^{-1}. The samples were prepared as suspensions of compound under study in petrolatum (Aldrich). **Electronic absorption spectra** (EAS) were registered on a Biowave II (Biochrom US, United States) spectrophotometer at 25°C and fluorescence spectra, on a Cary Eclipse (Agilent Technologies, United States) fluorescence spectrometer. Dynamic light scattering analysis was performed on a Delsa™ Nano (Beckman Coulter, Inc., United States) zeta potential and particle size analyzer; particle size distribution was studied on a Nicomp 380 (Particle Sizing Systems, United States) submicron particle size autocorrelation spectrophotometer.

Electron microscopy images were obtained with a Jeol 100CX (Japan) electron microscope at a magnification of 10000 or 20000×. NMR spectra were registered on a MSL-200 (Bruker, Germany) impulse Fourier transform spectrometer at a working frequency of 300.13 MHz. The measurements are reported as chemical shifts in δ, ppm, with respect to the internal standard (tetramethylsilane) in $CDCl_3$ or DMSO-d_6 as solvents. Mass spectra were recorded using a 1100 LCMSD (Agilent Technologies) instrument equipped with an atmospheric pressure chemical ionization (APCI) mass spectrometry detector and diode array UV detector (DAD).

Tetraphenylporphyrin (**I**) and porphyrins (**II**)–(**IV**) were synthesized according to published techniques [24, 25]. Compound (**V**) was synthesized by monopyrrole condensation in aqueous micellar medium [28].

Synthesis of 5-{4-2-[2-(2-Methoxyethoxy)-Ethoxy]oxyphenyl}-10,15,20-Tris(4-Hydroxyphenyl)porphyrin (V)

1-(4-Methylsulfonyl)-3,6,9-trioxodecane. Solution of triethylene glycol monomethyl ether (0.012 mol, 2.0 g) and triethylamine (0.18 mol, 18.20 g) in 50 mL of dry methylene chloride were cooled on ice and mixed under argon flow. Mesyl chloride (0.06 mol, 6.87 g) was added to the mixture dropwise during 30 min and mixed at room temperature for 24 h. The precipitate was filtered off and washed with methylene chloride to wash off the product from the filter. Filtrate was washed with water; the organic phase was separated and concentrated under vacuum. The product was purified from admixtures with chromatography on silica gel G 60 (eluent: methylene chloride–methanol, 20 : 1). Yield 2.32 g (79%). $R_f = 0.4$ (CH_2Cl_2 : MeOH = 20 : 1). ^{1}H NMR (DMSO-d_6): 4.48 (2 H, m, –$\underline{CH_2}$-OSO_2), 3.85 (2 H, m, –$\underline{CH_2}CH_2$-OSO_2), 3.73 (2 H, m, –$\underline{CH_2}OCH_2CH_2$-$OSO_2$), 3.68 (2 H, m, $\underline{CH_2}CH_2OCH_2CH_2$-$OSO_2$), 3.61 (2 H, m, $CH_3OCH_2\underline{CH_2}$–), 3.51 (2 H, m, $CH_3O\underline{CH_2}CH_2$-), 3.42 (3 H, s, $\underline{CH_3}O$–), 3.35 (3 H, s, CH_3SO_2-). ^{13}C NMR (DMSO-d_6): 37.19, 58.4, 68.55, 69.3, 70.4, 71.4.

4-{2-[2-(2-methoxyethoxy)ethoxy]ethoxy}benzaldehyde (VI). Triethylene glycol mesylate 3.72 mmol, 0.90 g) was added to a solution of *p*-hydroxybenzaldehyde (2.50 mmol, 0.30 g) in 15 mL DMF in the presence of cesium carbonate (1.63 g), and the mixture was stirred at 100°C for 14 h. The product was

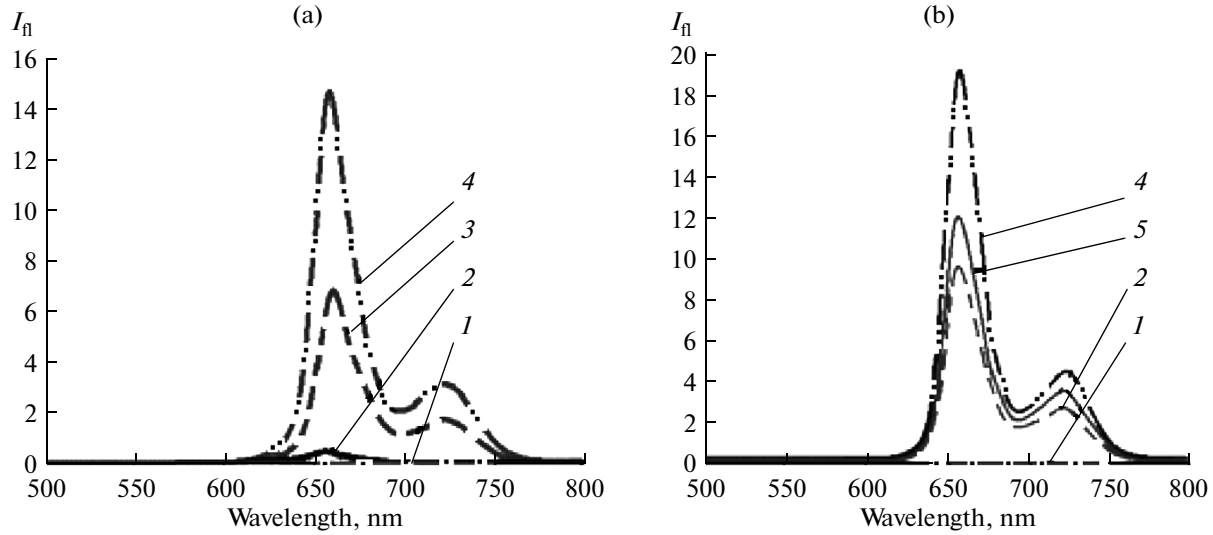

Fig. 3. Fluorescence spectra of SANPs loaded with (a) 2% CHS: *1*, buffer; *2*, porphyrin (**V**) concentration of 0% (control); *3*, 10%; and *4*, 5%; or (b) 2% porphyrin (**V**): *1*, buffer; *2*, CHS concentration of 0% (control); *5*, 1%; and *4*, 5%.

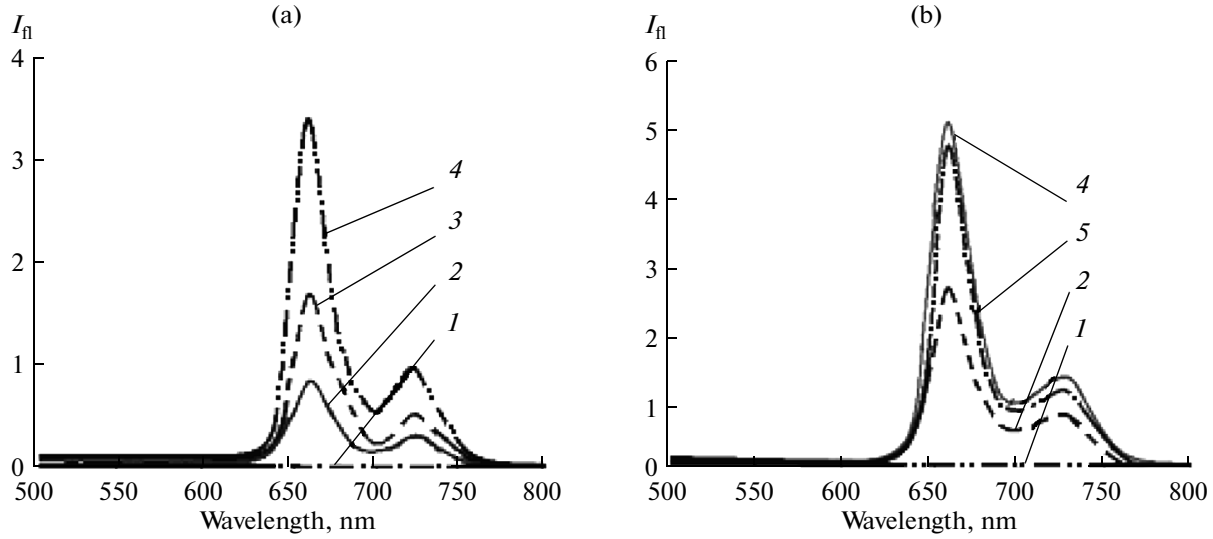

Fig. 4. Fluorescence spectra of SANPs loaded with (a) 2% CHS: *1*, buffer; *2*, porphyrin (**IV**) concentration of 0% (control); *3*, 10%; and *4*, 5%; or (b) 2% porphyrin (**IV**): *1*, buffer; *2*, CHS concentration of 0% (control); *5*, 1%; and *4*, 5%.

extracted and purified by column chromatography on silica gel G 60 (eluent: methylene chloride–ethyl acetate, 5 : 1). Yield 0.595 g (85%). R_f 0.55 (ethyl acetate). ^{1}H NMR (DMSO-d_6): 10.04 (1 H, s, C<u>H</u>O), 8.42 (2 H, m, Ar H2-H6), 7.30 (2 H, m, Ar H3-H5), 4.40 (2 H, m, ArOC<u>H$_2$</u>CH$_2$-), 3.96 (2 H, m, ArOCH$_2$C<u>H$_2$</u>-), 3.79 (2 H, m, -C<u>H$_2$</u>O(CH$_2$)$_2$OCH$_3$), 3.72–3.67 (4 H, m, -C<u>H$_2$</u>OC<u>H$_2$</u>CH$_2$OCH$_3$), 3.61 (2 H, m, -CH$_2$C<u>H$_2$</u>OCH$_3$), 3.40 (3 H, s, OC<u>H$_3$</u>). MS, *m/z*: 268.7 $[M]^+$, calculated 268.3 ($C_{14}H_{20}O_5$).

5-{4-2-[2-(2-Methoxyethoxy)-ethoxy]oxyphenyl}-10,15,20-tris(4-hydroxyphenyl)porphyrin (V). One mmol pyrrole (0.070 g), 0.25 mmol (0.067 g) 4-{2-[2-(2-methoxyethoxy)ethoxy]ethoxy}benzaldehyde, and 0.75 mmol (0.092 g) mmol *p*-hydroxybenzaldehyde were added to 0.5 M SDS aqueous solution (10 mL) and the mixture was stirred for 20 min under argon flow; then, 2% hydrochloric acid (150 μL) was added as a catalyst. After 1 h, oxidation with DDQ (0.220 g) was performed. Potassium hydroxide (2 M, 5 mL), 5 mL 1 M potassium phosphate, 10 mL 3 M potassium chloride, and 30 mL water were added to the reaction mixture. The product was extracted with ethyl acetate and, after the solvent was evaporated, purified by chromatography on silica gel G 60 (eluent: methylene chloride–ethyl acetate, 2 : 1). Yield of compound (**V**) 16.5 mg (8%). ^{1}H NMR (DMSO-d_6): 9.00 (6 H, d, H2, H8, H12, H13, H17, H18, J = 2.93 Hz),

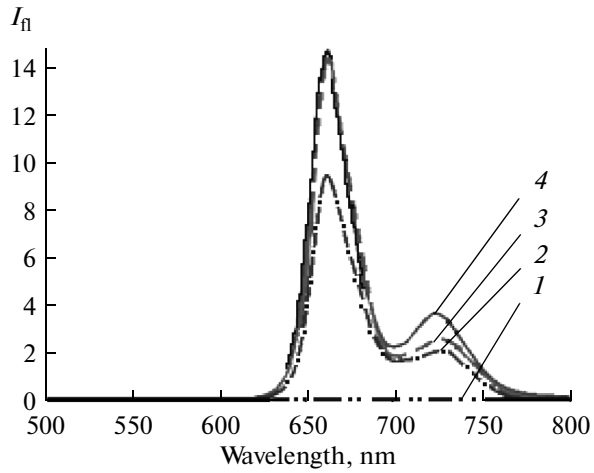

Fig. 5. Fluorescence spectra of porphyrin (**V**) at concentration of 2% (0.01 mg/mL) in THF (*3*), 2% in SANPs (*2*), and after the addition of 0.4 M SDS to sample *2*. *1*, 0% porphyrin (control).

8.96 (2 H, d, H3, H7, $J = 4.77$ Hz), 8. 22 (2 H, d, Ar H2, $J = 8.44$ Hz), 8.14 (6 H, d, Ar H2, $J = 24.94$ Hz), 7.48 (2 H, d, Ar H3, $J = 8.92$), 7.35 (6 H, d, Ar H3, $J =$ 8.25 Hz), 4.47 (2 H, m, -O-C$\underline{H}_2$), 4.03 (2 H, m, -O-$CH_2C\underline{H}_2$), 3.83 (2 H, m, $O(CH_2)_2OC\underline{H}_2$), 3.75 (2 H, m, $C\underline{H}_3O(CH_2)_2OC\underline{H}_2$-), 3.71 (2 H, m, $CH_3OCH_2\underline{CH}_2$), 3.62 (2 H, m, CH_3O-$\underline{CH}_2$), 3.39 (3 H, s, $C\underline{H}_3O$). ^{13}C NMR (DMSO-d_6: 158.35, 157.38, 135.47, 133.59, 131.83, 131.07, 130.52, 120.04, 119.23, 113.90, 112.95, 71.30, 70.01, 69.07, 67.39, 35.75, 30.75. MS, *m/z*: 825.9 [M + H], calculated 824.9 ($C_{51}H_{44}N_4O_7$). EAS (ethyl acetate), λ_{max}, nm ($\varepsilon \times 10^{-3}$, M^{-1} cm^{-1}): 418.0 (428), 515.8 (19.6), 552.6 (9.9), 592.4 (6.5), 650.6 (4.7).

Preparation of Spherical Amorphous Nanoparticles from BTM and Porphyrins

The size of SANPs was estimated with turbidimetry and dynamic light scattering. Zeta potential of the nanoparticles was measured by electrophoretic light scattering. Nanodispersion stability was evaluated by the rate of the nanoparticle sedimentation upon centrifugation. Nanoparticle morphology was determined by electron microscopy images obtained with negative staining with 1% aqueous solution. In a 100-mL round-bottom flask, solutions of BTM in THF (1 mL, 5 mg/mL) and porphyrin in THF (1 mg/mL) were mixed. To stabilize the SANP membrane and study the stability, cholesteryl hemisuccinate (CHS) in THF (1 mg/mL) was added. Two series of experiments were performed:

(a) at fixed concentration of porphyrin solution in THF (2% to the BTM mass; 0.1 mL, 1 mg/mL) and varying concentration of CHS solution in THF (0, 1, and 5% to the BTM mass) and

(b) at fixed concentration of CHS solution in THF (2% to the BTM mass; 0.1 mL, 1 mg/mL) and varying concentration of porphyrin solution in THF (5 and 10% to the BTM mass).

Phosphate buffer (25 mL; pH 7.5, 10 mM) was added to the mixture with a pipette upon intensive stirring, and the dispersion was stirred for 7 min at room temperature. The solvent was removed on a rotary evaporator at 35°C till the final volume reached 10 mL. Concentrated dispersions were centrifuged to remove the sediment.

ACKNOWLEDGMENTS

The work was supported by the Russian Foundation for basic Research (project no. 13-03-12046-ofi_m) and the Ministry of Education and Science of the Russian Federation.

REFERENCES

1. Balen, P., Martinet, M.C., Caron, G., Bouchard, G., Reist, M., Carrupt, P.-A., Fruttero, R., Gasco, A., and Testa, B., *Med. Res. Rev.,* 2004, vol. 24, pp. 299–324.
2. Zhu, C., Liu, L., Yang, Q., Lu, F., and Wang, S., *Chem. Rev.,* 2012, vol. 112, no. 8, pp. 4687–4735.
3. Soini, A.E., Yashunsky, D.V., Meltola, N.J., and Ponomarev, G.V., *Luminescence*, 2003, vol. 18, pp. 182–192.
4. Sezgin, Z., Yuksel, N., and Baykara, T., *Int. J. Pharmaceutics,* 2007, vol. 332, pp. 161–167.
5. Torchilin, V.P., *Pharm. Res.*, 2007, vol. 24, pp. 1–16.
6. Kuruppuarachchi, M., Savoie, H., Lowry, A., Alonso, C., and Boyle, R.W., *Mol. Pharmaceutics*, 2011, vol. 8, pp. 920–931.
7. Mojzisova, H., Bonneau, S., and Brault, D., *Eur. Biophys. J.,* 2007, vol. 14, pp. 943–953.
8. Caminos, D.A. and Durantini, E.N., *Bioorg. Med. Chem.*, 2006, vol. 14, pp. 4253–4259.
9. Sibrian-Vazquez, M., Jensen, T.J., and Vicente, M.G.H., *J. Photochem. Photobiol. B*, 2007, vol. 86, pp. 9–21.
10. Vargas, A., Pegaz, B., Debefve, E., Konan-Kouakou, Y., Lange, N., Ballini, J.-P., Bergh, H., Gurny, R., and Delie, F., *Int. J. Pharmaceutics*, 2004, vol. 286, pp. 131–145.
11. Ballut, S., Naud-Martin, D., Loock, B., and Maillard, P., *Org. Chem.*, 2011, vol. 76, pp. 2010–2028.
12. Nishiyama, N., Stapert, H.R., Zhang, G.-D., Takasu, D., Jiang, D.-L., Nagano, T., Aida, T., and Kataoka, K., *Bioconjugate Chem.*, 2003, vol. 14, pp. 58–66.
13. Kramer-Marek, G., Serpa, C., Szurko, A., Widel, M., Sochanik, A., Snietura, M., Kus, P., Nunes, R.M.D., Arnaut, L.G., and Ratuszna, A., *J. Photochem. Photobiol. B*, 2006, vol. 84, pp. 1–14.
14. Králová, J., Bríza, T., Moserová, I., Dolenský, B., Vašek, P., Poučková, P., Kejik, Z., Kaplánek, R., Martásek, P., Dvořak, M., and Král, V., *J. Med. Chem.*, 2008, vol. 51, pp. 5964–5973.
15. Králová, J., Kejík, Z., Bríza, T., Poučková, P., Král, A., Martásek, P., and Král, V., *J. Med. Chem.*, 2010, vol. 53, pp. 128–138.

16. Kępczyński, M., Nawalany, K., Jachimska, B., Romek, M., and Nowakowska, M., *Colloids Surf. B*, 2006, vol. 49, pp. 22–30.
17. Grin, M.A., Mironov, A.F., and Shtil, A.A., *Anti-Cancer Agents*, 2008, vol. 8, pp. 683–697.
18. Grin, M.A., Lonin, I.S., Likhosherstov, L.M., Novikova, O.S., Plyutinskaya, A.D., Plotnikova, E.A., Kachala, V.V., Yakubovskaya, R.I., and Mironov, A.F., *J. Porphyrins Phthalocyanines*, 2012, vol. 16, pp. 1094–1109.
19. Otsuka, H., Nagasaki, Y., and Kataoka, K., *Adv. Drug Delivery Rev.*, 2003, vol. 55, no. 3, pp. 403–419.
20. Hamblin, M.R., Miller, J.L., Rizvi, I., Loew, H.G., and Hasan, T., *Br. J. Cancer*, 2003, vol. 89, pp. 937–943.
21. Wiehe, A., Shaker, Y.M., Brandt, J.C., Mebs, S., and Senge, M.O., *Tetrahedron*, 2005, vol. 61, pp. 5535–5564.
22. Kaplun, A.P., Bezrukov, D.A., Popenko, V.I., and Shvets, V.I., *Biofarm. Zh.*, 2011, vol. 3, no. 2, pp. 28–40.
23. Kaplun, A.P. and Pakhar'kova, N.I., Poruchikova (Gavrilova), L.A., Bezrukov, D.A., Popenko, V.I., and Shvets, V.I., *Vestnik MITKhT*, 2010, vol. 5, no. 2, pp. 73–75.
24. Lindsey, J.S., Hsu, H.C., and Schreiman, I.C., *Tetrahedron Lett.*, 1986, vol. 27, no. 41, pp. 4969 – 4970.
25. Bragina, N.A., Mishkina, K.A., Formirovskii, K.A., and Mironov, A.F., *Makrogeterotsikly*, 2011, vol. 4, no. 2, pp. 116–121.
26. Nawalany, K., Kozik, B., Kepczynski, M., Zapotoczny, S., Kumorek, M., Nowakowska, M., and Jachimska, B., *J. Phys. Chem. B*, 2008, vol. 112, pp. 12231–12239.
27. Zhao, X. and Janda, K.D., *Tetrahedron Lett.*, 1997, vol. 38, no. 31, pp. 5437–5440.
28. Bonar-Law, R.P., *Org. Chem.*, 1996, vol. 61, pp. 3623–3634.

Translated by N. Kuznetsova